JOURNAL OF GEOPHYSICAL RESEARCH: ATMOSPHERES, VOL. 118, 11,534–11,545, doi:10.1002/jgrd.50645, 2013

Relationships between the large-scale atmosphere and the small-scale convective state for Darwin, Australia

L. Davies,[1] C. Jakob,[2] P. May,[3] V. V. Kumar,[3] and S. Xie[4]

Received 6 March 2013; revised 10 July 2013; accepted 10 July 2013; published 25 October 2013.

[1] A persistent problem for numerical weather and climate models is the representation of tropical convective precipitation which for the most part occurs on spatial and temporal scales too small and too short to be explicitly resolved. Given that model parameterizations represent this subgrid convection as a function of the large-scale atmospheric state, an understanding of the strongest relationships between the two scales is needed. This study introduces a method to create two concurrent long-term data sets that describe both the large-scale atmosphere and the characteristics of the small-scale convection. Important relationships between these two scales are then investigated. It is found that convective precipitation, through convective precipitation area, has the strongest relationship with dynamical variables such as moisture convergence and vertical velocity at midlevels. The magnitude of the fluctuations of convective strength about the mean is found to be anticorrelated with the strength of the large-scale variables, indicating a more stochastic behavior of tropical convection in weakly than strongly forced regimes, respectively. Atmospheric stability related variables are not found to be positively related to either convective precipitation area or convective precipitation intensity, which is often an assumption made in convective parameterization. On the contrary, in a more unstable atmosphere, there is lower convective precipitation.

Citation: Davies, L., C. Jakob, P. May, V. V. Kumar, and S. Xie (2013), Relationships between the large-scale atmosphere and the small-scale convective state for Darwin, Australia, *J. Geophys. Res. Atmos.*, *118*, 11,534–11,545, doi:10.1002/jgrd.50645.

1. Introduction

[2] Atmospheric convection is an important phenomenon which drives weather and climate in the tropics as well as the global general circulation. Convection is relevant on a range of spatial and temporal scales from large-scale phenomena, such as the Inter-Tropical Convergence Zone, El Nino-Southern Oscillation, and the Madden-Julian Oscillation, to short weather time scales, such as an individual squall line and mesoscale convective systems. Numerical models exhibit limitations in their ability to capture convective phenomena. Particular examples include biases in the tropical mean precipitation distribution [*Sun et al.*, 2006; *Zhang et al.*, 2007] and significant timing errors in the diurnal cycle of convection over land [*Yang and Slingo*, 2001]. Shortcomings in model simulations have been related to the model representation of convection [e.g., *Neale et al.*, 2008; *Bechtold et al.*, 2008; *Zhang et al.*, 2006; *Neale and Slingo*, 2003; *Wang and Schlesinger*, 1999]. This is largely due to the limitations of the convective parameterizations used in models to represent the subgrid scale behavior of convection in relation to the resolved large-scale processes. Accurate representation of convection is particularly important for the tropics where precipitation is generally associated with convective cloud systems.

[3] Convective parameterizations (see *Arakawa* [2004] for a full review of convective parameterization approaches) generally exploit some relationship between the large-scale, given by the atmospheric state at the model grid box scale, and the convective scale. The schemes mostly invoke an assumption that the two scales are in quasi-equilibrium [*Arakawa and Schubert*, 1974; *Emanuel*, 1991; *Brown and Bretherton*, 1997] and use these assumptions to provide closure to the model equations. A variable which characterizes the thermodynamic state of the atmosphere, such as Convectively Available Potential Energy (CAPE), is often used to determine convective strength. CAPE is the vertical integral of the temperature perturbation of a buoyant air parcel ascending from near the surface to its level of neutral buoyancy. A comprehensive investigation of other possible relationships, between a large range of large-scale and small-scale variables, which may be used in the closure of convective parameterizations is somewhat lacking.

[1]School of Mathematics, Monash University, Melbourne, Victoria, Australia.
[2]ARC Centre of Excellence for Climate System Science, Monash University, Melbourne, Victoria, Australia.
[3]Centre for Australian Weather and Climate Research, Bureau of Meteorology, Melbourne, Victoria, Australia.
[4]Atmospheric Sciences Division, Lawrence Livermore National Laboratory, Livermore, California, USA.

Corresponding author: L. Davies, School of Earth Sciences, The University of Melbourne, Melbourne 3010, Victoria, Australia. (laura.davies@unimelb.edu.au)

2169-897X/13/10.1002/jgrd.50645

[4] Another possible limitation of convective parameterizations (and other parameterizations in general) is that they determine the subgrid scale convective behavior deterministically, meaning that for a given large-scale state, only one possible convective state can be attained. This is unlikely to be true in the real atmosphere, but traditional parameterizations cannot produce variability about their mean relationship between the two scales. Several cloud-resolving models (CRM) studies have identified variability in the large to small-scale relationships, however, to our knowledge there are no observational studies investigating the stochastic nature of these relationships [e.g., *Cohen and Craig*, 2006; *Shutts and Palmer*, 2007; *Plant and Craig*, 2008]. There have been several attempts to include stochastic elements in the description of convection in models. *Buizza et al.* [1999] showed that applying multiplicative noise to the physics tendencies improved modeled skill. *Lin and Neelin* [2007] used empirical relationships to adjust the convective parameterization. *Khouider and Majda* [2006] used a Markov chain lattice to stochastically describe the evolution of convective cloud types in a model grid-cell. *Plant and Craig* [2008] developed a fully stochastic convective parameterization. These studies have used either assumptions of empirical relationships or higher resolution models, such as CRM, to study the stochastic nature of the relationships. This study aims to supplement this earlier work by providing observations of the key relationships and also quantifying their stochastic components.

[5] In this study, we first develop two concurrent data sets, one representing the large-scale atmosphere and another the small-scale convective state, over a sufficiently long time period to sample a large range of different states. These data sets are then used to investigate important relationships between the two scales and furthermore to determine the stochastic nature of the relationships. Section 2 describes the methodology used to derive data sets for the large-scale atmospheric state and the concurrent small-scale convective state. Section 3 then discusses some key relationships between the two scales that are relevant for convective parameterizations. The stochastic nature of these relationships is probed in section 4. The following sections then discuss the results (section 5) and summarize the main conclusions (section 6).

2. Deriving Concurrent Long-Term Large-Scale Atmospheric and Convective States

[6] To investigate relationships between the large-scale atmospheric state and associated convection, two concurrent data sets are required, one that describes the average state of the atmosphere over an area similar to that of a Global Climate Model (GCM) grid-box and another that describes the subgrid-scale behavior of convection. In order to investigate a wide range of meteorological conditions and to increase sampling, these data sets should be as long as possible. This section describes the derivation of two such data sets for a tropical location, i.e., Darwin, Australia.

2.1. The Large-Scale State for a Tropical Location

[7] In order to study convection, the large-scale state data set should, ideally, include both thermodynamic and dynamic variables with a high degree of accuracy. An important source of such large-scale state data sets are the observations made during the intensive observation periods of field experiments such as TOGA-COARE: (Tropical Ocean-Global Atmosphere-The Coupled Ocean-Atmosphere Response Experiment) and Global Atmospheric Research Program's Atlantic Tropical Experiment (GATE) [*Webster and Lukas*, 1992; *Houze Jr and Betts*, 1981]. Such studies often deploy arrays of radiosonde observations and collect surface and top of the atmosphere data including energy and water fluxes. A useful method to analyze this data is the variational budget analysis developed by *Zhang and Lin* [1997] where radiosonde, top of the atmosphere (TOA), and surface data are combined and constrained by the vertically integrated heat and moisture budgets. *Zhang et al.* [2001] showed that surface precipitation data significantly improved the quality of the analysis. While field experiments produce the most comprehensive data sets to study tropical convection, they are usually of short duration, which prevents a large-sample statistical analysis of the relationship between convection and the large-scale state of the atmosphere. The top panel of Figure 1 shows an example of the results from such a field experiment. It shows the time-height evolution of vertical motion during the recent Tropical Warm Pool-International Cloud Experiment (TWP-ICE) at Darwin, Australia [*May et al.*, 2008] as derived by the variational analysis technique described above [*Xie et al.*, 2010]. It can be seen that there is strong upward motion during the active monsoon period (before day 25 which is 25 January 2006). A subsequent suppressed monsoon period is associated with downward motion between 700 and 200 hPa and toward the end of the TWP-ICE period (after day 33 which is 3 February 2006), the diurnal cycle becomes dominant with frequently alternating upward and downward motion.

[8] A source of long-term large-scale data sets is operational or reanalyses of the atmosphere as provided by several numerical weather prediction (NWP) centers. Such data sets cover many years and in principle provide a good source of large-scale information. However, analysis techniques in the tropics are not as far advanced as those in the extratropics and the lack of dynamical constraints, as well as the increased role of diabatic processes, limits the accuracy of the resulting analysis products. This is exemplified by the middle panel of Figure 1 which shows vertical motion for TWP-ICE from the European Centre for Medium-Range Weather Forecasts (ECMWF) operational analysis. It shows upward motion during the active monsoon consistent with the observations, although the vertical structure differs somewhat. It appears the timing of peak precipitation lags the observations, and this behavior is discussed in *Petch et al.* [2013]. During the suppressed period, the analysis fails to show the midlevel downward motion (compare to the observations, top panel) and the diurnally driven period is not well captured.

[9] To exploit both the strengths of the variational analysis technique and to overcome some of the weaknesses of NWP analysis results, a hybrid approach was developed by *Xie et al.* [2004]. NWP analysis is used as a replacement for radiosonde observations which provides higher temporal resolution sounding data than the twice daily long-term observations available. The analysis data are combined with surface and TOA observations at the Atmospheric Radiation

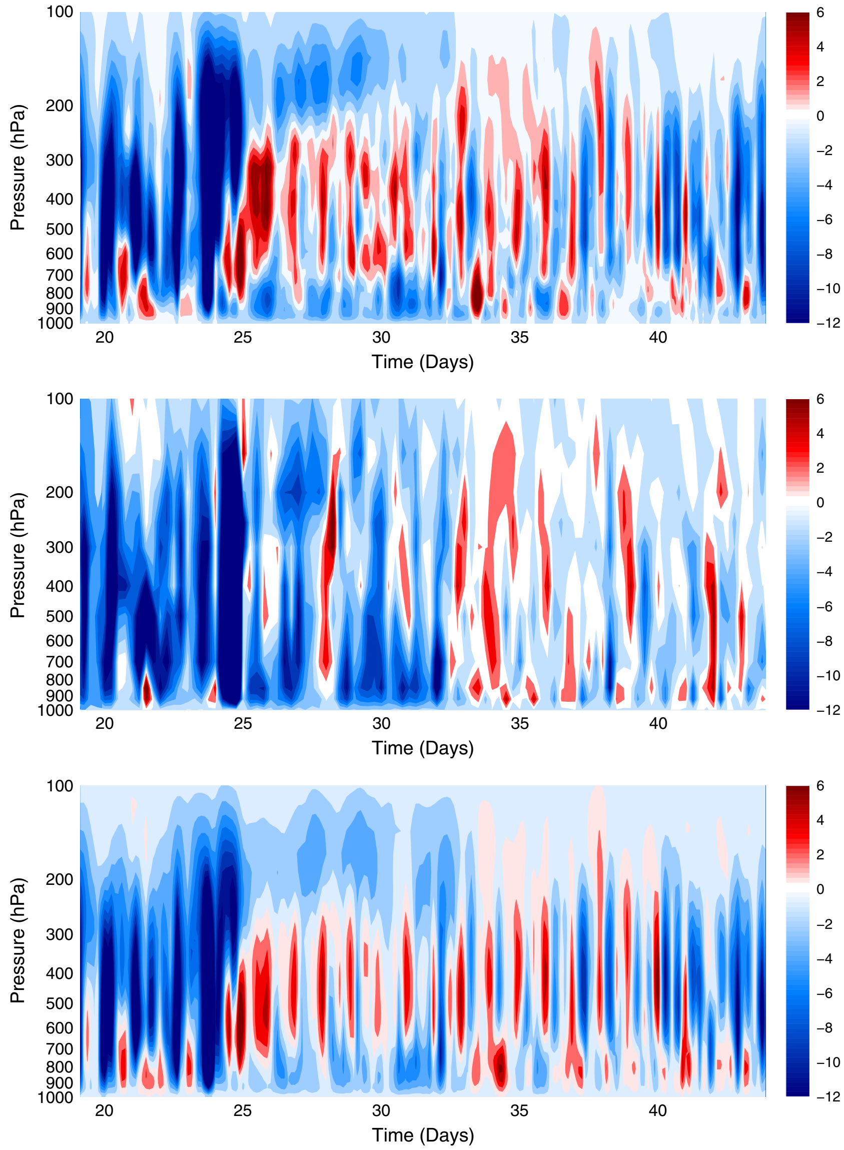

Figure 1. Timeseries of vertical profiles of vertical velocity in pressure coordinates (omega) using all observations, i.e., (top panel) the best-estimate values as described in *Xie et al.* [2010], (middle panel) the direct ECMWF analysis, and (bottom panel) using the hybrid approach described here. Data are shown for the TWP-ICE period (19 January–14 February 2006) at Darwin, Australia.

Measurement site at the U.S. Southern Great Plains using the variational analysis technique of *Zhang and Lin* [1997]. The surface data are radar-derived precipitation rates, and TOA microwave radiometer total column water vapor is used to constrain the moisture budget. *Xie et al.* [2004] demonstrated that for this extratropical location, the hybrid approach can successfully provide large-scale state data for long, continuous periods of time. The key observations for using this technique are long-term observations for surface precipitation and TOA radiation.

[10] We apply the hybrid approach to the TWP-ICE period so that its results can (i) be compared with the full field-experiment data and (ii) be evaluated against the ECWMF analysis to gauge any improvement over a pure NWP system. To do so, ECMWF analysis grid-points around Darwin are used to replace the TWP-ICE radiosonde observations. Specifically, the vertical profiles of zonal and meridional winds, temperature, and specific humidity are interpolated to the locations of the radiosonde launch sites. The method used was Barnes interpolation, however, experimentation with bilinear interpolation suggests that the resulting profiles are not sensitive to the method used.

[11] The bottom panel of Figure 1 shows vertical velocity derived using the hybrid technique. During the active period, vertical motion is similar to when using all observations, in particular the timing of the peak vertical motion is improved compared to the ECMWF analysis (middle panel). During the suppressed period, the hybrid approach shows downward motion in midlevels. Although the structure is somewhat different to using all observations, it resembles the observations (top panel). At the end of the TWP-ICE period, there is correctly intermittent upward and downward motion.

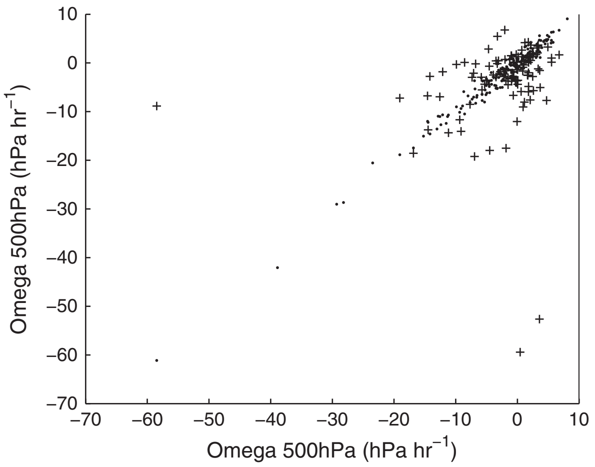

Figure 2. Relationship of 500 hPa vertical velocity in pressure coordinates (omega) derived using the variational approach from all observations on the *x* axis against both omega at 500 hPa from ECMWF analysis shown as crosses and 500 hPa omega derived using the variational method but using the hybrid approach (as discussed in the text) shown as points. Data are shown for the TWP-ICE period (19 January–14 February 2006) at Darwin, Australia.

[12] Figure 2 compares vertical velocity at 500 hPa derived with variational analysis using the hybrid approach and the ECMWF analysis to vertical velocity at 500 hPa derived with variational analysis from all observations. It is clear that when using the hybrid approach, the representation of vertical velocity substantially improves compared to the ECMWF analysis. Correlating all observed values of vertical velocity at 500 hPa with those derived from the hybrid approach and the ECMWF analysis yields correlation coefficients of 0.98 and 0.25, respectively.

[13] Having demonstrated the utility of the hybrid approach in providing reliable estimates of large-scale information, we apply the technique to derive three wet seasons (2004/2005, 2005/2006, and 2006/2007) of the large-scale state information for the TWP-ICE region around Darwin. The analysis technique is limited to periods, such as the wet season, when there are sufficient observations of precipitation. This data set is derived using the ECMWF operational analysis as radiosonde surrogate and constraining the variational analysis with area-mean surface precipitation derived from the polarimetric C-band radar (CPOL) [*Keenan et al.*, 1998] using the algorithm of *Bringi et al.* [2004]. It is worth noting that the use of the area-mean total precipitation as a constraint in the variational analysis limits its use as a surrogate for convective activity below. The radar data are processed in the same way as during the TWP-ICE experiment [see *Xie et al.*, 2010 for more detail]. The resulting data set has approximately 1900 samples at 6-hourly intervals.

2.2. Defining the Concurrent Convective State

[14] To correctly associate a particular large-scale atmospheric condition with a convective state, a description of the latter is also required concurrent in space and time with the large-scale state. To achieve this, a detailed analysis of the CPOL observations at 2.5 km above the surface is performed. Firstly, the data are classified into its convective and stratiform components using the algorithm of *Steiner et al.* [1995]. This method classifies pixels with large values of radar reflectivity as convective and then associates sufficiently intense, nearby precipitation values as also convective. Other precipitating radar pixels are classified as stratiform. The classified data are then area-averaged over the 6 h periods which are ± 3 h the time of the large-scale state to produce convective and stratiform precipitation rates. Precipitation rates are further decomposed into area and intensity as given by $P = \sigma I$, where P is precipitation, σ is precipitation area, and I is precipitation intensity (defined as precipitation per unit precipitation area), for the same 6 h periods. Additional information on the small-scale state is found by analyzing the statistics of convective cells using the Thunderstorm Identification, Tracking, Analysis, and Nowcasting (TITAN) radar data analysis tool [*Dixon and Wiener*, 1993] which identifies characteristics of individual convective storms. Further detail on this analysis can be found in *Kumar et al.* [2012].

[15] While the focus of this study is on how the convective scale variables relate to the large scale, it is worthwhile determining how the small-scale variables relate to each other. Table 1 shows correlations coefficients between the small-scale variables related to both the convective and stratiform parts of the precipitation processes. Domain-averaged total precipitation is strongly correlated with both convective precipitation (through convective precipitation area) and stratiform precipitation. This result may be related to the finding of *Mapes et al.* [2006] who suggested that convective and stratiform precipitation exhibit similar relationships over different spatial and temporal scales. Total precipitation area is very strongly correlated with stratiform precipitation area as stratiform precipitation dominates the areal coverage. While both convective and stratiform

Table 1. Summary of Correlations Between Small-Scale Precipitation Variables

	Precipitation Area	Convective Precipitation	Convective Precipitation Area	Precipitation Stratiform	Stratiform Precipitation Area	Convective Precipitation Intensity	Stratiform Precipitation Intensity
Precipitation	0.85	0.94	0.93	0.94	0.81	0.50	0.44
Precipitation area	1.00	0.65	0.71	0.93	0.99	0.34	0.23
Convective precipitation		1.00	0.96	0.75	0.61	0.57	0.49
Convective precipitation area			1.00	0.79	0.66	0.52	0.49
Stratiform precipitation				1.00	0.92	0.37	0.33
Stratiform precipitation area					1.00	0.31	0.20
Convective precipitation intensity						1.00	0.88

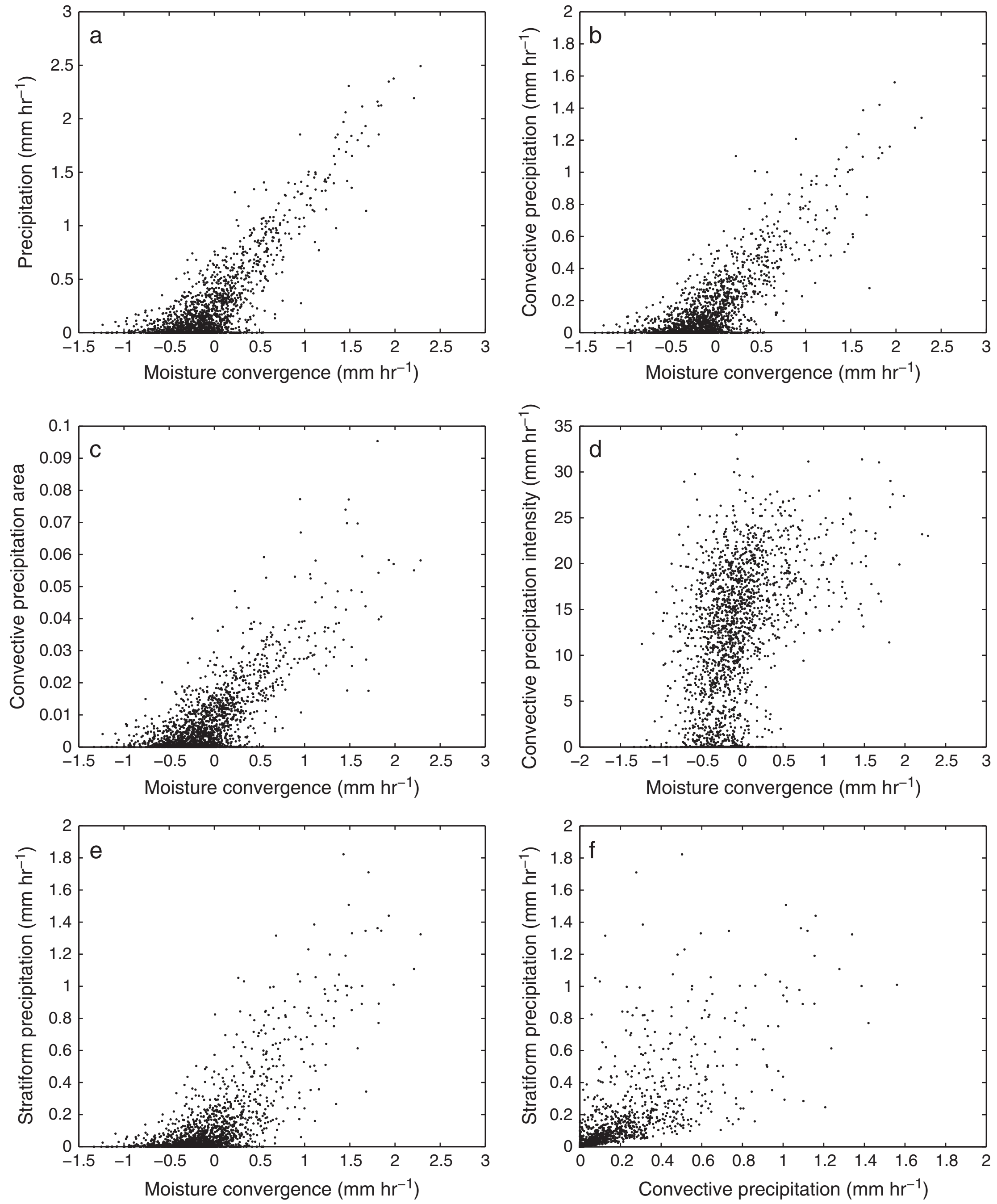

Figure 3. Relationship of moisture convergence with (a) precipitation, (b) convective precipitation, (c) convective precipitation area fraction, (d) convective precipitation intensity, and (e) stratiform precipitation. (f) Relationship of convective precipitation and stratiform precipitation.

precipitation are strongly correlated with their precipitation areas (0.96 and 0.92, respectively), there is weaker correlation (0.75) between convective and stratiform precipitation components. Convective and stratiform precipitation are also less related to the other's area (0.61 and 0.79, respectively). While there is some relationship between convective intensity and stratiform intensity (0.88 correlation), there are weak correlations with all other precipitation and area variables. Further investigation attributes this to complex nonlinearities in the relationships (cf. section 3). Convective precipitation, which is dominated by convective precipitation area, and convective precipitation intensity are key variables for convective parameterizations. These small-scale variables form the main basis for further analysis in the subsequent sections.

3. Relationships Between the Large-Scale Atmospheric State and Convection

[16] We now use the two concurrent data sets described in section 2 to investigate relationships between the large- and the small-scale states, i.e., between atmospheric

Table 2. Summary of Correlations Between Moisture Convergence and Omega at 700 hPa and Various Small-Scale Convective Precipitation Terms

	Moisture Convergence	Omega (700 hPa)
Precipitation	0.81	–0.79
Precipitation area	0.65	–0.61
Convective precipitation	0.78	–0.76
Convective precipitation area	0.75	–0.76
Convective precipitation intensity	0.45	–0.39

dynamics/thermodynamics and convection. Given the possible large number of large-scale variables, the investigation is divided to three overall categories, dynamics, thermodynamics, and atmospheric stability.

3.1. Relationships Involving Dynamical Processes

[17] This section investigates the relationships of the convective state to a few dynamical characteristics of the large-scale state. Specifically, the dynamical variables considered are vertically integrated moisture convergence and vertical velocity in pressure coordinates (ω). Figure 3 shows the relationships between some key small-scale variables and moisture convergence, and Table 2 shows the associated correlations. While moisture convergence is a vertically integrated variable, it is found to be strongly correlated with vertical motion at 700 hPa (–0.69). Precipitation is highly correlated with both dynamical variables, with this correlation being slightly higher for moisture convergence (0.81) compared to ω at 700 hPa (–0.79). Figure 3a shows that indeed the largest precipitation occurs with the strongest moisture convergence. While there is generally lower precipitation associated with negative moisture convergence, precipitation can occur when there is net divergence and hence likely subsiding condition due to shallow but precipitating convective clouds. There is scatter about this relationship particularly for low values of moisture convergence.

[18] This data set does not allow for the interpretation of causality as convective heating and precipitation are known to induce moisture convergence, and equally under conditions of high moisture convergence, convection is more likely. This issue of cause and effect has been discussed in the context of the assumptions made in convective parameterizations e.g., *Arakawa* [2004], and it has been argued [*Emanuel*, 1994] that convergence is a consequence, rather than a cause, of convection. Investigation shows that the relationship between convective precipitation and the dynamical variable at the previous 6 h interval is somewhat weaker (0.30 for moisture convergence and –0.27 for ω at 700 hPa). This issue will be discussed further in section 5.

[19] It is worth noting again that a strong relationship between total precipitation and large-scale vertical motion is expected as a result of the use of total precipitation in the construction of the large-scale data set. Hence, further analysis will focus on variables that are not a direct input to the variational analysis scheme used here.

[20] In section 2.2, we showed that there are strong relationships between total precipitation and both convective precipitation and convective precipitation area. It is therefore not surprising that the relationship existing between moisture convergence and total precipitation is also apparent with convective precipitation and convective precipitation area (Figures 3b and 3c; Table 2). The correlations are slightly weaker, however, 0.78 and 0.75, respectively. This suggests that larger moisture convergence is associated with increased convective precipitation through predominantly increasing the convective precipitation area. The same applies to ω at 700 hPa although correlations are lower. This result provides observational support for a finding from cloud-resolving modeling studies, e.g., *Cohen and Craig* [2006], that convection responds to an increase in prescribed model "forcing" predominantly through an increase in convective area. Figure 3d and Table 2 show that the relationship is different when considering convective precipitation intensity. There is little discernible relationship between moisture convergence and precipitation intensity, although large values of moisture convergence tend to produce intensities above 10 mm h^{-1}, and negative moisture convergence results in a wide range of lower precipitation intensities. This complex interaction results in low correlations between the large-scale atmospheric state and precipitation intensity and may be related the dependence of precipitation intensity on raindrop terminal velocity [*Parodi and Emanuel*, 2009].

[21] As shown in Table 1, there is a strong correlation between total precipitation and stratiform precipitation. Therefore, stratiform precipitation is also strongly correlated with moisture convergence (Figure 3e) and ω at 700 hPa (0.75 and –0.71, respectively), although the correlation is weaker than with convective precipitation. Such a relationship exists as there is a strong relationship between convective and stratiform precipitation (Figure 3f and Table 2) which may be expected as convection is the source of stratiform cloud in many cases. For this reason, we focus on convective characteristics hereon.

3.2. Relationships Involving Moisture

[22] This section investigates the relationship of convective-scale behavior in relation to large-scale moisture. Specifically, the large-scale moisture variable considered is midlevel moisture which is defined as the specific humidity at 600 hPa. Similar relationships are observed with other moisture variables, for example, midlevel moisture is correlated 0.96 with column-integrated relative humidity and 0.95 with precipitable water. Also, as there are strong relationships between precipitation, convective precipitation, and convective precipitation area, which are also apparent in the relationships with large-scale variables (cf. sections 2.2 and 3.1), this section will focus on convective precipitation area and convective precipitation intensity only.

[23] Figure 4 shows the relationship between midlevel moisture and small-scale convective variables. While there is a general tendency for larger convective precipitation area in moister atmospheres, there is much scatter in that relationship. Essentially, atmospheres which are more moist support large convective areas with a small increase in the likelihood of large area with increased moisture. There are two possible reasons for this (i) because the atmosphere is moist, the effects of entrainment on convective strength are reduced leading to more convective precipitation or (ii) in a strongly convecting atmosphere, evaporation of both precipitation and detrained condensate will moisten

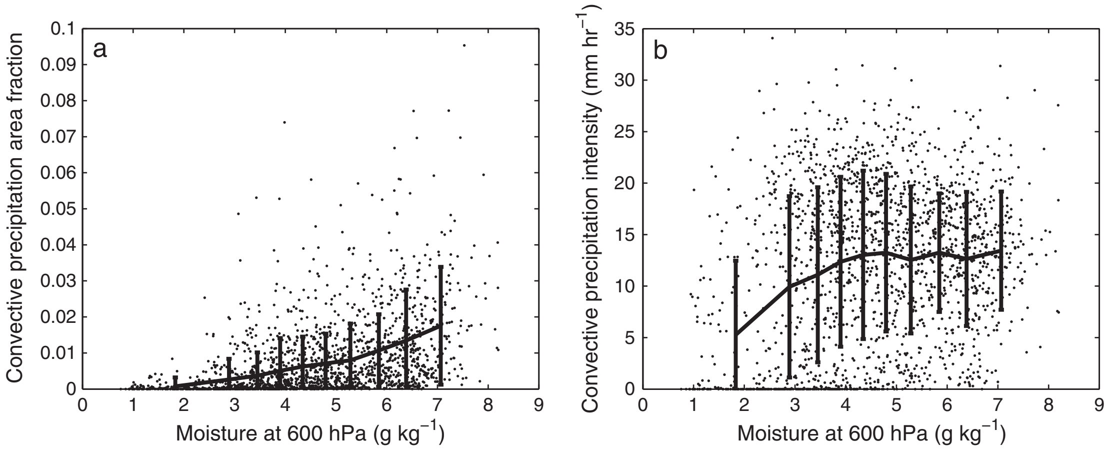

Figure 4. Relationship of 600 hPa moisture with (a) convective precipitation area fraction and (b) convective precipitation intensity. Also shown are mean and ± 1 standard deviation values for deciles of the data set.

the atmosphere. This result does not suggest causality but shows that a weak relationship exists. Figure 4a, using convective precipitation area rather than total precipitation, somewhat resembles distributions in *Bretherton et al.* [2004] and *Holloway and Neelin* [2009] with increasing precipitation area for larger values of moisture. However, the relationship does not have the strong pickup in precipitation shown in *Holloway and Neelin* [2009] who used 1 h radiosonde data nor the more gradual increase *Bretherton et al.* [2004] found using daily data. Figure 4a shows that there is much scatter in the relationship between midlevel moisture and convective area consistent with the findings of *Peters and Neelin* [2006] who found an increase in precipitation variance for high values of precipitable water. The differences between the findings in this study and the results in previous studies may be somewhat explained by *Masunaga* [2012] who found that the timescales investigated were important when determining the nature of the relationship between precipitable water and precipitation. Figure 4b shows the perhaps surprising result that convective precipitation intensity does not show much discernible relationship with midlevel moisture, with the exception that in a very dry atmosphere domain-mean convective intensity is slightly lower. This implies that at least small but strong convective clouds can exist in any atmosphere and that once again, it is the area of convection that increases in atmospheres that are more moist.

[24] Figure 5 shows a different perspective on how convective precipitation relates to moisture. Here probability distributions of precipitation in convective cells from the TITAN analysis [*Kumar et al.*, 2012], averaged over 6 h, are shown as a function of midlevel (600 hPa) moisture. The precipitation distributions are sorted into deciles based on midlevel moisture and then averaged over each decile. Red colors represent averages with the largest moisture and blue colors averages with the low moisture. In general, many more convective cells are observed when the atmosphere is moist, thus reflecting the increased convective area shown in Figure 3. Therefore, for each decile, the distribution is normalized by the number of convective cells observed in that decile. When the atmosphere is moist, the numerous convective cells tend to have lower precipitation intensity. As the atmosphere dries, there is a shift in the distribution toward fewer convective cells but with larger values of precipitation intensity. This shows that in a moist atmosphere, convective cells are less intense, but more numerous; however, in a drier atmosphere, while there are fewer convective cells over all, the individual cells are more likely to be more intense.

3.3. Relationships Involving Atmospheric Stability

[25] This section will investigate the relationship of convective scale activity with two measures of atmospheric stability: Convective Available Potential Energy (CAPE), which is a vertically integrated measure of the buoyancy of a parcel lifted from 990 hPa, and a measure more frequently used by weather forecasters to predict convective showers and thunderstorms called the *K*-index [*Charba*, 1977].

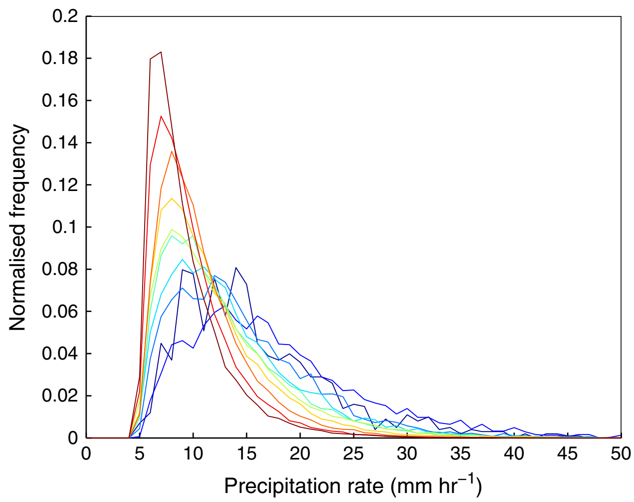

Figure 5. Distribution of precipitation rate per convective cell averaged over deciles of 600 hPa moisture. The distribution is normalized by the total number of convective cells in each decile. Deciles with large moisture are in red and deciles with low moisture are in blue.

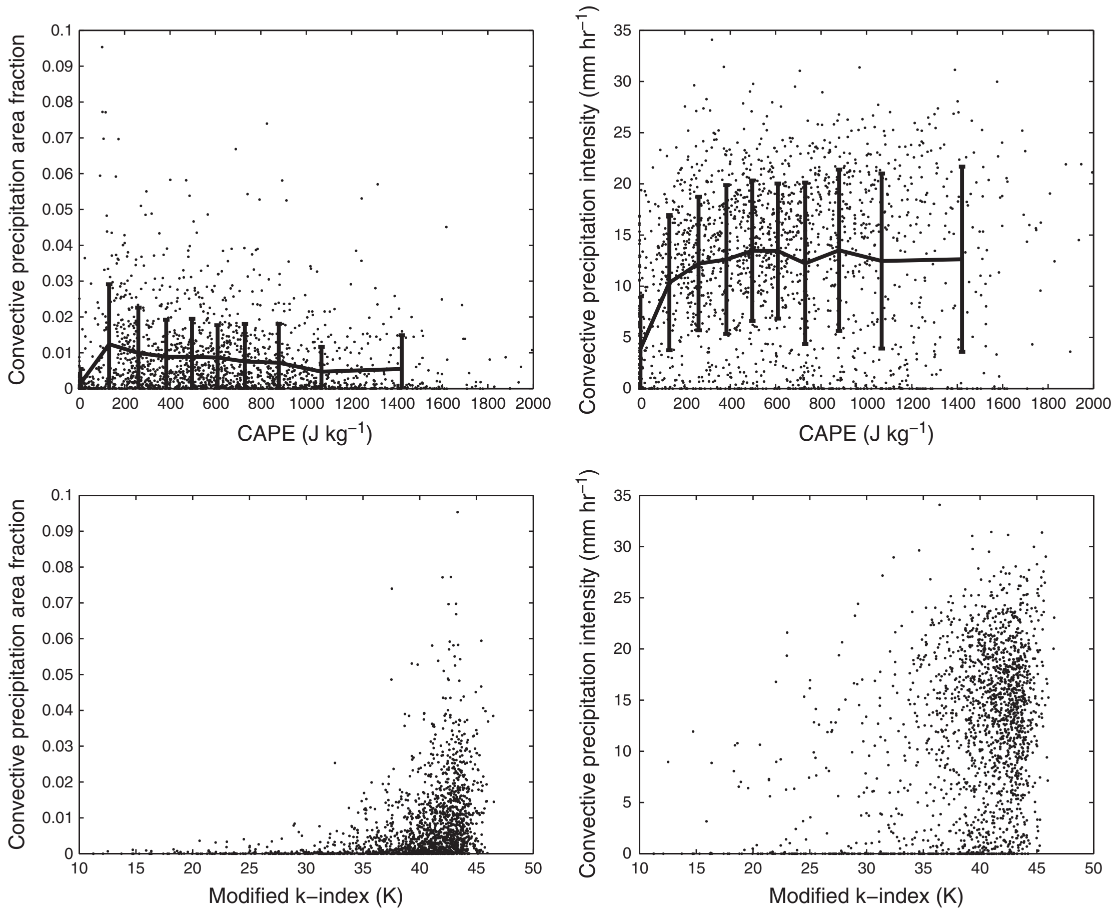

Figure 6. Relationship of (top) CAPE and (bottom) *K*-index with (left) convective precipitation area fraction and (right) convective precipitation intensity. In the top panels, also shown are mean and ±1 standard deviation values for deciles of the data set.

The *K*-index is calculated based on temperature (T) and dew point temperature (T_d) at key pressure levels as shown in equation (1).

$$K = \underbrace{\frac{T_{1000\ \mathrm{hPa}} + T_{850\ \mathrm{hPa}}}{2} - T_{500\ \mathrm{hPa}}}_{\text{(a)}} + \underbrace{\frac{T_{d,1000\ \mathrm{hPa}} + T_{d,850\ \mathrm{hPa}}}{2}}_{\text{(b)}} - \underbrace{(T_{700\ \mathrm{hPa}} - T_{d,700\ \mathrm{hPa}})}_{\text{(c)}} \quad (1)$$

[26] Figure 6 shows the relationships between CAPE, *K*-index, and selected small-scale variables. Convective precipitation and CAPE effectively have zero correlation (–0.003) showing that, at least for this data set, CAPE is not likely to be a good predictor of convective precipitation consistent with *McBride and Frank* [1999]. The relationship between CAPE and precipitation has been also discussed in *Xie and Zhang* [2000] and *Zhang* [2002]. CAPE at the previous 6 h interval has slight positive correlation with convective precipitation (0.06) which is discussed further in section 5. Detailed investigation shows that CAPE increases through a combination of an increased height of the level of neutral buoyancy and larger perturbations in the parcel temperature throughout the atmosphere compared to the environment. Convective precipitation intensity also does not have a strong relationship with CAPE.

[27] The *K*-index on the other hand has a very different relationship with convective precipitation. Figure 6 (bottom left) shows that convective precipitation values greater than 0.5 mm h^{-1} only occur for values of *K*-index greater than 35 K. Generally, in the forecasting context, *K*-index values greater than 30 K indicate potential of Mesoscale Convective Cloud (MCC) and greater than 40 K almost 100% chance of thunderstorms.

[28] Equation (1) indicates that the *K*-index has three distinct components. Term (a) relates to lower tropospheric stability, term (b), a measure of mean low-level (boundary layer) moisture, and finally, term (c) relates to midlevel humidity. Given that the *K*-index includes term (a), which is also relevant for CAPE, it is instructive to investigate which of these terms, if any, has the dominant role in determining the relationship to convective precipitation. Investigation shows that the stability component of the *K*-index (term a) has very similar relationship with convective precipitation to that of CAPE (Figure 6, top left). CAPE and the stability component of the *K*-index are correlated 0.7. The low-level moisture and midlevel humidity components of the *K*-index (terms b and c) are correlated 0.77 and 0.94, respectively, with the full *K*-index, rendering these terms important for determining the *K*-index values. The relationship between the humidity component of the *K*-index and convective precipitation, in particular, resembles Figure 4a.

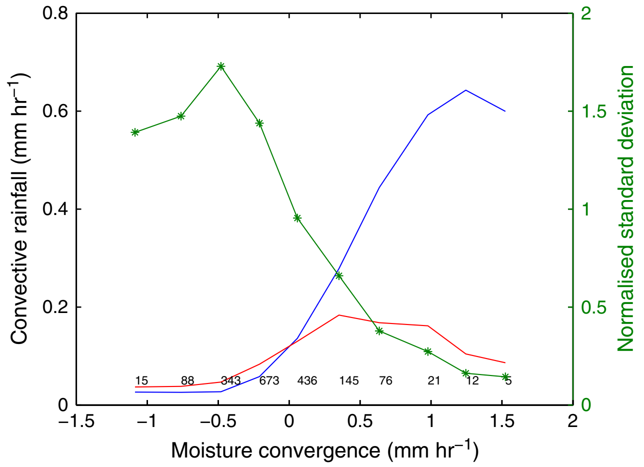

Figure 7. Mean and standard deviation 6 h mean convective precipitation (blue and red lines, respectively, and shown on left *y* axis) as a function of moisture convergence. The data are computed over 10 bins, and the number of points in each bin is shown above the *x* axis. Also shown is the ratio of the standard deviation to the mean (green line shown on the right *y* axis).

Hence, these terms of the *K*-index are the main contributors to the full *K*-index and when combined are correlated 0.96 with the full *K*-index. For this data set at least, the *K*-index is a predictor for precipitation based on low-level moisture and/or midlevel humidity rather than on estimate of atmospheric stability.

[29] Figure 6 (bottom right) shows that there is very little relationship between *K*-index and convective precipitation intensity. Large values of *K*-index tend to be associated with a range of convective precipitation intensities.

4. The Stochastic Nature of the Large-Scale to Small-Scale Relationships

[30] Section 3 has shown that there exist a number of relationships between the large-scale state of the tropical atmosphere and the state of convection. However, it was also shown that even the strongest of those relationships, such as that between moisture convergence and convective rainfall area, show a considerable amount of scatter, confirming the at least partially stochastic nature of small- to large-scale relationships. As the degree of stochastic behavior has significant consequences for the representation of small-scale processes such as convection in coarse-resolution (>10 km) models, it is worthwhile to try and further quantify some simple statistical properties of the relationships, which is the goal of this section.

[31] We choose the apparently strongest relationship, namely that between convective precipitation and moisture convergence (Figure 3b) for this investigation. First, the moisture convergence values are grouped into 10 equally-sized bins. Then, for each bin, we calculate the mean and standard deviation of its respective convective precipitation values. Figure 7 shows these quantities and also their ratio. The mean convective precipitation is low for small values of moisture convergence and increases with increasing values of moisture convergence. The standard deviation of convective precipitation also increases with increasing values of moisture convergence. It is clear that for negative values of moisture convergence, the standard deviation of convective precipitation is larger than the mean value suggesting that convective precipitation appears rather stochastic in weak dynamical conditions. For positive and increasing moisture convergence, the mean convective precipitation increases more rapidly than the standard deviation showing that larger values of convective precipitation are likely more deterministically related to the large scale. This is confirmed by the ratio of standard deviation to mean which is around 1.5 for negative values of moisture convergence and above 0.5 for large positive values of moisture convergence. This finding confirms the empirical fact that convective storms in the tropics are easier to predict when embedded into large-scale dynamical features, such as a monsoon trough or the active phase of the Madden-Julian Oscillation, than in weakly forced conditions.

[32] It is interesting to note that the nature of this relationship is not consistent with some existing implementations aimed at characterizing small-scale stochastic behavior in large-scale models, such as multiplicative noise [*Buizza et al.*, 1999; *Teixeira and Reynolds*, 2008] but rather that noise (or the stochastic behavior) decreases as a function of increasing forcing.

5. Discussion

[33] Results in the previous sections have shown that convective precipitation and in particular the area covered by convection are related to a number of characteristics of the large-scale state, in particular moisture convergence and midlevel vertical velocity. One caveat of this study is the location for which the data were available. Given the region around Darwin consists of both areas of land and areas of ocean, it is possible that there may be a strong diurnal component to the found relationships. In particular, the Tiwi Island have strong convective storms each afternoon which may contribute considerably to the total convective precipitation [*Keenan et al.*, 1990; *Crook*, 2001].

[34] The role of the diurnal cycle is further investigated by first calculating the mean diurnal cycle of vertical profiles of vertical velocity (ω). Then the mean diurnal cycle is removed from the timeseries of the vertical profiles of ω. Figure 8 shows the mean ω for deciles of convective precipitation. Red colors represent averages with the largest convective precipitation and blue colors averages with the low convective precipitation. The solid lines are without the diurnal cycle removed and the dotted lines after the diurnal component is removed. It can clearly be seen that the role of the diurnal cycle is to modify the structure of the vertical profiles rather than to significantly alter the magnitude or the relationship of vertical motion with convective precipitation. In fact, the correlations of convective precipitation and moisture convergence or ω at 700 hPa (with the diurnal cycle removed) are 0.77, and all correlations are similar to those in Table 2. Similar results are found when considering moisture and stability variables with the conclusion that the diurnal cycle does not substantially effect the relationships discussed in section 3. Another test for the robustness of the relationships is to divide the data set by wind direction, which in the Darwin region is well known to affect

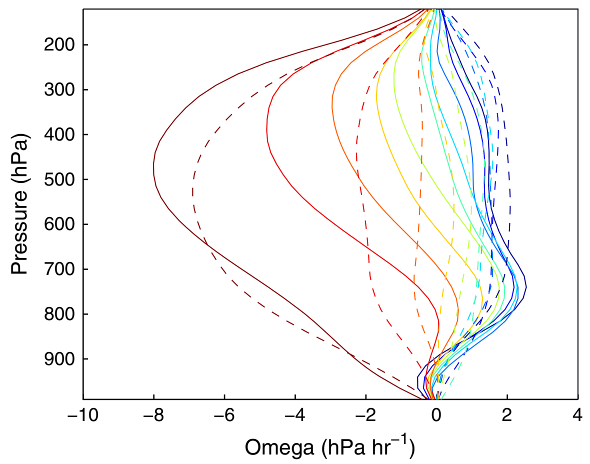

Figure 8. Profiles of vertical motion (omega) over the TWP-ICE domain averaged over deciles of 6 h mean convective precipitation. Deciles with strong precipitation are red and low convective precipitation are blue. The dashed lines show omega with the diurnal cycle removed.

the nature of the convection from more continental in easterly conditions to more oceanic in westerly conditions [*May et al.*, 2008]. There are no discernible differences in the large-to-small-scale relationships when doing so (not shown). Finally, preliminary investigations using similar data sets for another location, namely the largely land-free Kwajalein atoll, also confirm this result (not shown).

[35] As discussed in section 3.1, it is difficult to establish cause and effect relationships between convection and the atmospheric large-scale state from this data, it can only be shown that such relationships exist. For example, convection and moisture convergence are shown to be strongly related in this study and, although the relationship is weaker when considering the moisture convergence 6 h previous, there is still positive correlation. It is likely that, while convection can enhance convergence in a general sense, the relationship is more subtle than simply attributing either cause or effect to either moisture convergence or convection.

[36] An important factor to consider when interpreting the above results is the effect of the temporal resolution and the spatial averaging of the data set on the relationships identified. For example, the relationship between moisture convergence and convective precipitation (Figure 3b) shows that convective precipitation does occur under subsidence conditions. Given that the data are averaged over 6 h periods over a large area, it may be that subsidence does not occur for the whole period or at all locations. There may be localized convergence associated with the precipitation. Another interesting result is that this data set does not show strong relationship between convection and CAPE. The amount of convective precipitation at a grid box in a numerical model is often related to the strength of CAPE through the closure of the convective parameterization. These results, however, suggest the reverse is true, i.e., that convective precipitation is small when CAPE is large. This is understandable as CAPE suggests the presence of instability in the atmosphere; and should convection, and associated convective heating and precipitation develop, the instability would be reduced or removed. In fact, it may be more reasonable to consider that CAPE at some previous point in time might be a predictor for subsequent convective precipitation. This data set suggests a weak positive relationship between convection and CAPE, however, the 6 h temporal resolution of the data limits further detailed investigation of the relationship. Finally, over short-time periods and small spatial areas, convection dries the atmosphere by removing moisture through precipitation. The results here (section 3.2 and Figure 4a) that show that large convective precipitation is associated with large precipitable water may, again, be due to the low temporal resolution data, which is averaged over large areas.

6. Summary

[37] This study uses concurrent observations of the large-scale and convective scale state of the tropical atmosphere at Darwin, Australia to investigate the nature of the relationship between the two scales. It first presents an application of a hybrid approach for deriving the large-scale state of the atmosphere for a tropical location. Testing of the methodology for the period of the TWP-ICE experiment shows that constraining ECMWF analyses with observed precipitation improve the estimates of large-scale variables, such as vertical velocity, compared to the ECMWF analyses alone. It is shown that the hybrid data set is a close approximation of that derived using all observations from the field experiment. The concurrent data set describing the small-scale atmospheric state is derived through the analysis of CPOL radar observations. The radar-derived precipitation data is classified into convective and stratiform components. Complex relationships are found between the small-scale precipitation variables themselves. This study focuses on convective precipitation, convective precipitation area, and convective precipitation intensity as these are the first-order characteristics that need to be represented in convective parameterizations used in GCM. Their faithful representation is a prerequisite for describing the more complex interaction of convection with its associated stratiform cloud systems. It is found, averaged over a domain similar in size to a GCM grid box, that convective precipitation mainly increases through increasing the area that precipitates, which supports the findings of earlier CRM studies.

[38] Investigation into the relationships between the large- and the small-scale states shows that the strongest relationships of the convective scale are with dynamical variables such as moisture convergence or vertical velocity. While the issue of cause and effect cannot easily be separated, the data show clearly that strong convective precipitation is associated with positive moisture convergence while lower convective precipitation occurs under weak or divergence conditions. It is also shown that the stochastic nature of this relationship is dependent on the strength of the large-scale forcing, which is inconsistent with multiplicative noise used in some convective parameterizations. When convection is embedded in a strong dynamically active state, the relationship between the two is highly deterministic. In weak dynamical conditions, although convection is less active, there is much scatter in the relationship. In a relative sense, convection is therefore more stochastic when "weakly forced." This fact is well known to

forecasters in tropical regions when forecasting weather on a daily basis.

[39] Strong relationships with stability related variables, such as CAPE, are neither found with convective precipitation area nor convective precipitation intensity. The relationship identified suggests that when convective precipitation is large, CAPE is most likely to be small, although there is much scatter in the relationship. In fact, a model of convection based on CAPE would suggest a highly stochastic relationship which highlights a possible limitation of current deterministic convective parameterization that are based on CAPE closures.

[40] This study shows that the construction of a high quality long-term data set describing the large-scale atmosphere at a tropical location is possible. In addition to NWP analysis data, the method requires frequent radar observations to calculate precipitation and related small-scale variables. Such data sets can be used to investigate the fundamental relationships between convection and the large-scale atmosphere. Furthermore, where relationships are identified, their deterministic or stochastic nature can be determined. Such data sets provide valuable observational evidence to develop convective parameterizations.

[41] **Acknowledgments.** Davies and Jakob are supported by the Office of Science (BER), U.S. Department of Energy under grant DE-SC0002731.

[42] The contributions of S. Xie to this work were performed under the auspices of the U. S. Department of Energy (DOE), Office of Science, Office of Biological and Environmental Research by Lawrence Livermore National Laboratory under contract DE-AC52-07NA27344 and supported by the Atmospheric Radiation Measurement Program of the Office of Science at the DOE.

References

Arakawa, A. (2004), The cumulus parameterisation problem: Past, present and future, *J. Atmos. Sci.*, *17*(13), 2493–2525.

Arakawa, A., and W. Schubert (1974), Interaction of a cumulus cloud ensemble with the large-scale environment, Part1, *J. Atmos. Sci.*, *31*, 674–701, doi:10.1175/1520-0469(1974)031<0674:IOACCE>2.0.CO;2.

Bechtold, P., M. Köhler, T. Jung, F. Doblas-Reyes, M. Leutbecher, M. J. Rodwell, F. Vitart, and G. Balsamo (2008), Advances in simulating atmospheric variability with the ECMWF model: From synoptic to decadal time-scales, *Q. J. R. Meteorol. Soc.*, *134*(634), 1337–1351.

Bretherton, C. S., M. Peters, and L. Black (2004), Relationships between water vapor path and precipitation over the tropical oceans, *J. Clim.*, *17*, 1517–1528.

Bringi, V., T. Tang, and V. Chandrasekar (2004), Evaluation of a new polarmetrically based Z-R relation, *J. Atmos. Oceanic Technol.*, *21*, 612–623.

Brown, R. G., and C. Bretherton (1997), A test of the strict quasi-equilibrium theory on long time and space scales, *J. Atmos. Sci.*, *54*, 624–638.

Buizza, R., M. Miller, and T. N. Palmer (1999), Stochastic representation of model uncertainties in the ECMWF ensemble prediction system, *Q. J. R. Meteorol. Soc.*, *125*, 2887–2908.

Charba, J. P. (1977), *Operational System for Predicting Thunderstorms Two to Six Hours in Advance*, National Weather Service, NOAA.

Cohen, B., and G. Craig (2006), Fluctuations in an equilibrium convective ensemble. Part II: Numerical experiments, *J. Atmos. Sci.*, *63*, 2005–2015.

Crook, N. A. (2001), Understanding Hector: The dynamics of island thunderstorms, *Mon. Weather Rev.*, *129*(6), 1550–1563.

Dixon, M., and G. Wiener (1993), TITAN: Thunderstorm identification, tracking, analysis, and nowcasting-A radar-based methodology, *J. Atmos. Oceanic Technol.*, *10*(6), 785–797.

Emanuel, K. (1991), A scheme for representing cumulus convection in large-scale models, *J. Atmos. Sci.*, *48*(21), 2313–2329.

Emanuel, K. A. (1994), *Atmospheric Convection*, 1st ed., Oxford University Press.

Holloway, C. E., and J. D. Neelin (2009), Moisture vertical structure, column water vapor, and tropical deep convection, *J. Atmos. Sci.*, *66*(6), 1665–1683.

Houze Jr, R. A., and A. K. Betts (1981), Convection in gate, *Rev. Geophys.*, *19*(4), 541–576.

Keenan, T., B. Morton, X. S. Zhang, and K. Nyguen (1990), Some characteristics of thunderstorms over Bathurst and Melville Islands near Darwin, Australia, *Q. J. R. Meteorol. Soc.*, *116*(495), 1153–1172.

Keenan, T. D., K. Glasson, F. Cummings, T. S. Bird, J. Keller, and J. Lutz (1998), The BMRC/NCAR C-band polarimetric (CPOL) radar system, *J. Atmos. Oceanic Technol.*, *15*, 871–886.

Khouider, B., and A. Majda (2006), Multicloud convective parametrizations with crude vertical structure, *Theor. Comput. Fluid Dyn.*, *20*, 351–375.

Kumar, V. V., A. Protat, P. T. May, C. Jakob, G. Penide, S. Kumar, and L. Davies (2012), On the effects of large-scale environment and surface types on convective cloud characteristics over Darwin, Australia, *Mon. Weather Rev.*, *141*, 1358–1374.

Lin, J., and J. Neelin (2007), Toward stochastic deep convective parameterization in general circulation models, *Geophys. Res. Lett.*, *30*(4), 1162, doi:10.1029/2002GL016203.

Mapes, B., S. Tulich, J. Lin, and P. Zuidema (2006), The mesoscale convection life cycle: Building block or prototype for large-scale tropical waves? *Dyn. Atmos. Oceans*, *42*, 3–29.

Masunaga, H. (2012), Short-term versus climatological relationship between precipitation and tropospheric humidity, *J. Clim.*, *25*, 7983–7990.

May, P. T., J. H. Mather, G. Vaughan, C. Jakob, G. M. McFarquhar, K. N. Bower, and G. G. Mace (2008), The tropical warm pool international cloud experiment, *Bull. Am. Meteorol. Soc.*, *89*, 629–645.

McBride, J. L., and W. M. Frank (1999), Relationships between stability and monsoon convection, *J. Atmos. Sci.*, *56*, 2436.

Neale, R., and J. Slingo (2003), The maritime continent and its role in the global climate: A GCM study, *J. Clim.*, *16*(5), 834–848.

Neale, R. B., J. H. Richter, and M. Jochum (2008), The impact of convection on ENSO: From a delayed oscillator to a series of events, *J. Clim.*, *21*(22), 5904–5924.

Parodi, A., and K. Emanuel (2009), A theory for buoyancy and velocity scales in deep moist convection, *J. Atmos. Sci.*, *66*(11), 3449–3463.

Petch, J., A. Hill, L. Davies, A. Fridlind, C. Jakob, Y. Lin, S. Xie, and P. Zhu (2013), Evaluation of intercomparisons of four different types of model simulating TWP-ICE, *Q. J. R. Meteorol. Soc.*, doi:10.1002/qj.2192.

Peters, O., and J. D. Neelin (2006), Critical phenomena in atmospheric precipitation, *Nat. Phys.*, *2*, 393–396.

Plant, R. S., and G. C. Craig (2008), A stochastic parameterization for deep convection based on equilibrium statistics, *J. Atmos. Sci.*, *65*, 87–105.

Shutts, G., and T. Palmer (2007), Convective forcing fluctuations in a cloud-resolving model: Relevance to the stochastic parameterization problem, *J. Clim.*, *20*, 187–202.

Steiner, M., R. Houze, and S. Yuter (1995), Climatological characterisation of three-dimensional storm structure from operational radar and rain gauge data, *J. Appl. Meteorol.*, *34*, 1978–2007.

Sun, Y., S. Solomon, A. Dai, and R. W. Portmann (2006), How often does it rain?, *J. Clim.*, *19*(6), 916–934.

Teixeira, J., and C. A. Reynolds (2008), Stochastic nature of physical parameterizations in ensemble prediction: A stochastic convection approach, *Mon. Weather Rev.*, *136*(2), 483–496.

Wang, W., and M. E. Schlesinger (1999), The dependence on convection parameterization of the tropical intraseasonal oscillation simulated by the UIUC 11-layer atmospheric GCM, *J. Clim.*, *12*(5), 1423–1457.

Webster, P., and R. Lukas (1992), TOGA-COARE: The coupled ocean-atmosphere response experiment, *Bull. Am. Meteorol. Soc.*, *73*(9), 1377–1416.

Xie, S., R. T. Cederwall, and M. Zhang (2004), Developing long-term single-column model/cloud system - resolving model forcing data using numerical weather prediction products constrained by surface and top of the atmosphere observations, *J. Geophys. Res.*, *109*, D01104, doi:10.1029/2003JD004045.

Xie, S., T. Hume, C. Jakob, S. A. Klein, R. B. McCoy, and M. Zhang (2010), Observed large-scale structures and diabatic heating and drying profiles during TWP-ICE, *J. Clim.*, *23*, 57–79.

Xie, S., and M. Zhang (2000), Impact of the convection triggering function on single-column model simulations, *J. Geophys. Res.*, *105*(D11), 14–983.

Yang, G. Y., and J. Slingo (2001), The diurnal cycle in the tropics, *Mon. Weather Rev.*, *129*, 784–801.

Zhang, C., M. Dong, S. Gualdi, H. H. Hendon, E. D. Maloney, A. Marshall, K. R. Sperber, and W. Wang (2006), Simulations of the Madden–Julian oscillation in four pairs of coupled and uncoupled global models, *Clim. Dyn.*, *27*(6), 573–592.

Zhang, G. J. (2002), Convective quasi-equilibrium in midlatitude continental environment and its effect on convective parameterization, *J. Geophys. Res.*, *107*(D14), doi:10.1029/2001JD001005.

Zhang, M. H., and J. L. Lin (1997), Constrained variational analysis of sounding data based on column integrated budgets of mass, heat, moisture, and momentum: Approach and application to ARM measurements, *J. Atmos. Sci.*, *54*, 1503–1524.

Zhang, M. H., J. L. Lin, R. T. Cederwall, J. J. Yio, and S. C. Xie (2001), Objective analysis of ARM IOP data: Method and sensitivity, *Mon. Weather Rev.*, *129*, 295–311.

Zhang, X., W. Lin, and M. Zhang (2007), Toward understanding the double intertropical convergence zone pathology in coupled ocean-atmosphere general circulation models, *J. Geophys. Res.*, *112*, D12102, doi:10.1029/2006JD007878.